

DTI and Quantitative Histological Correlation of Diffuse Fibrosis in Failing Hearts

Osama Abdullah¹, Stavros G Drakos², Abdallah Kfoury³, Joseph Stehlik⁵, Craig H. Selzman³, Bruce B Reid³, Nikolaos A Diakos², Kim Brunisholz³, Divya Ratan Verma³, Omar Wever-Pinzon³, Craig Myrick⁴, Dean Y Li², and Edward W Hsu¹

¹Bioengineering, University of Utah, Salt Lake City, UT, United States, ²Molecular Medicine Program, University of Utah, UT, United States, ³UTAH Cardiac Transplant Program, UT, United States, ⁴Intermountain Donor Services, UT, United States

Introduction. Diffuse fibrosis of the failing heart impacts the mechanical (1) and electrical (2) behaviors of the myocardium, and has been linked to increased risk of ventricular and atrial tachyarrhythmia and sudden cardiac death (3). T1-mapping before and after gadolinium (Gd) administration is currently used to quantify extracellular space volume fraction as a surrogate for diffuse myocardial fibrosis (4). However, in light of recent concerns on Gd-based contrast agent use (5), alternative techniques for quantifying diffuse myocardial fibrosis can be desirable. Diffusion tensor imaging (DTI) has been used to characterize tissue microstructure including mapping the fiber structure of the myocardium (6,7). Although the technique is increasingly employed clinically to evaluate myocardial remodeling associated with cardiac diseases (8,9), quantitative correlation between DTI-derived scalar metrics and diffuse fibrosis remains lacking. The present study aims to investigate the relationship and underlying biophysical basis between DTI parameters and diffuse myocardial fibrosis.

Methods. Human failing heart specimens (n=14) and control hearts (n=5) were obtained from patients with end-stage heart failure due to idiopathic dilated cardiomyopathy and donors who died from non-cardiac causes, respectively, and fixed in 10% formalin prior to imaging. DTI was performed on a Bruker 7T scanner using a standard diffusion weighted spin echo sequence: 2000 ms TR, 30 ms TE, 64 x 64 matrix, 1.5 mm in-plane resolution, 4 slices of 1.0 mm slice thickness, 12 optimized diffusion encoding directions at 1500 s/mm² b-value, and 1 non-weighted (B0) image. The average signal to noise ratio of the B0 images was 84. DTI diffusivities (in ranked order) D₁, D₂, D₃, mean diffusivity (MD) and fractional anisotropy (FA) indices were calculated and averaged over the entire myocardial area. Collagen content was quantified from Masson's Trichrome-stained histological sections by calculating the percent area of blue-staining pixels. Student t-tests were applied to compare same measurements between the two groups, and Pearson's correlation coefficients were computed between DTI parameters and collagen content.

To better understand the origin and behavior of the observed DTI parameters, computational analysis was conducted based on observed DTI properties of the normal myocardium and those previously reported for collagenous tissues (10), using both "slow" and "fast exchange" compartmental models (11). Monte Carlo simulations (12) were performed to examine the dependence of DTI parameters on collagen content and effects of image noise.

Results. Figure 1 shows representative DTI and histological images obtained in the present study. The group-averaged measurements shown in Table 1 indicate that all diffusivity parameters except for D₁ are significantly increased, and that the FA is significantly decreased in failing hearts. Pearson correlations reveal moderate but significant correlation between collagen content with all parameters, except for D₁. Figure 2 shows that the computational compartmental analyses are highly consistent with experimental observations. Little difference was seen between simulation results obtained using slow and fast exchange models. The simulations also predicted that the changes of the transverse diffusivities are greater than D₁, and that noise impacts FA more than any other DTI parameter (not shown).

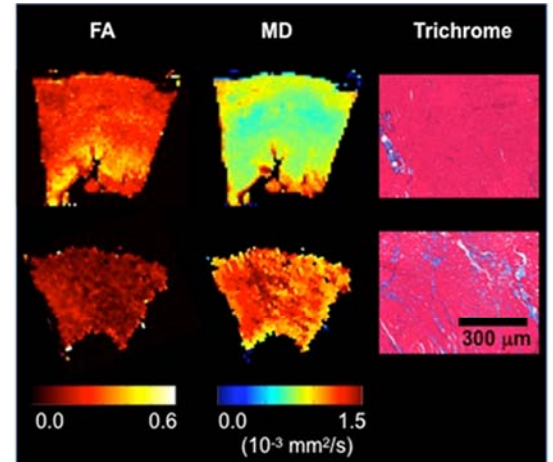


Figure 1. DTI and Trichrome-stained histology images from typical normal (top) and failing (bottom) heart specimens.

Table 1. Scalar DTI parameters and collagen content obtained from failing and control normal hearts. Pearson correlation coefficient (*r*) is reported between the DTI parameters and collagen content.

Parameter	Control	Failing	Change	Pearson <i>r</i>
D ₁	0.88±0.02	0.93±0.02	6%	0.46
D ₂	0.64±0.01	0.73±0.02	14%*	0.56*
D ₃	0.51±0.02	0.63±0.02	24%*	0.62*
MD	0.68±0.01	0.76±0.02	12%*	0.59*
FA	0.27±0.02	0.21±0.01	-22%*	-0.51*
Collagen	7.1 ± 1.1	19.4 ± 2.0	171%*	---

*P<0.05; diffusivities are in 10⁻³ mm²/s; collagen is in percent area.

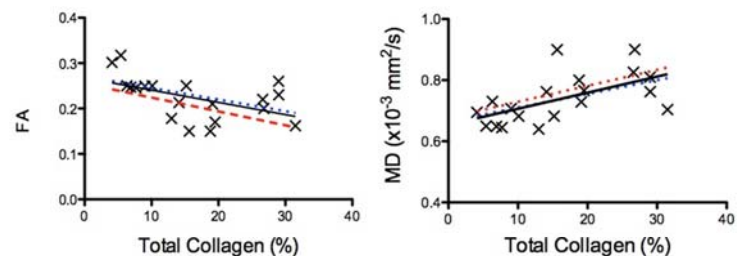


Figure 2. Scatter plots of FA and MD with collagen content. Experimental data (x) are shown along their linear regression fit (solid) and simulated behaviors under fast (dotted red) and slow (dotted blue) exchange bi-compartmental models.

Discussion and Conclusions. Experimental results indicate that myocardial fibrosis in failing hearts leads to increased water diffusivity and decreased anisotropy, which are consistent with previous observations in cardiac ischemia via DTI (8). Moreover, the degrees of correlation between the DTI parameters and collagen content are comparable to those previously reported for T1-mapping with contrast enhancement (13). The largest DTI parameter changes are observed for the transverse diffusivities, especially D₃, indicating that the metric may be better suited for quantifying fibrosis than the more commonly used FA and MD. The trends and magnitudes of DTI parameter changes are well explained by compartmental exchange of diffusion between myocardial and collagenous tissues. Given the recent technical advances and increasing use of *in vivo* cardiac DTI, these findings suggest a potential role for DTI in evaluating the tissue microstructural remodeling in failing hearts.

References: [1] Tamaki S; *PLoS One*. 2013; 8:e68893. [2] Ten Tusscher KHJ; *Europace*. 2007; 9 Suppl 6:vi38–45. [3] Bohl S; *Heart. Lung Circ*. 2010; 19:117–32 [4] Jellis C; *J. Am. Coll. Cardiol*. 2010; 56:89–97. [5] Marckmann P; *J. Am. Soc. Nephrol*. 2006; 17:2359–62. [6] Bassar PJ; *Biophys. J*. 1994; 66:259–67. [7] Hsu EW; *Am J Physiol Heart Circ Physiol*. 1998; 274:H1627–34. [8] Wu M-T; *Circulation*. 2006; 114:1036–45. [9] McGill L-A; *J. Cardiovasc. Magn. Reson*. 2012; 14:86. [10] Henkelman RM; *Magn. Reson. Med*. 1994; 32:592–601. [11] Niendorf T; *Magn. Reson. Med*. 1996; 36:847–57. [12] Pierpaoli C; *Magn Reson Med*. 1996; 36:893–906. [13] Messroghli D; *Circ Cardiovasc Imaging*. 2011; 4:636–40.

Acknowledgment: This work was supported by NIH R01 HL092055.